bias

Bremer Institut für
angewandte Strahltechnik

F. Vollertsen, T. Seefeld (Eds.)

Thermal Forming

Proceedings of the IWOTE'05:
1st International Workshop on
Thermal Forming

Bremen, Germany, April 13-14, 2005

The publishers assume no responsibility for any errors or omissions, which might occur in papers printed in this volume. The authors, which are named in the contents, have sole responsibility for the papers.

Thermal Forming
Frank Vollertsen, Thomas Seefeld (Eds.)

Strahltechnik Volume 26, BIAS Verlag, Bremen, 2005
Editors of the series: F. Vollertsen, W. Jüptner

ISBN: 3-933762-16-2

Print: DiguPrint Digitaldruck- und Offsetdruck-Service, Bochum
Printed in Germany

Micro adjustment by thermal upsetting

Jacek Widłaszewski

Institute of Fundamental Technological Research, Polish Academy of Sciences
Ul. Świętokrzyska 21, Warsaw, 00-049, Poland

Thermal strain produced by local heating of miniature metal components is already applied for adjustment in mass production in the electronic industry. Non-contact and forceless adjustment, alignment or trimming of sub-assemblies by use of a well-defined heat source, like the laser beam, allows for product miniaturisation and automation of manufacturing. However, the implemented procedures of adjustment by thermal forming are based on experimental investigations and numerical simulations, what makes it difficult to perform optimisation of the component design and processing parameters. The paper presents analytical-numerical modelling of thermal deformations induced to small metal frame structure. Experimental verification was performed using Nd:YAG laser beam. Theoretical model is based on one-dimensional heat flow solution. Thermo-elastic and thermo-plastic deformations are described. Derived formulae allow for optimisation of the considered structure and of the adjustment process.

1 Introduction

Thermal upsetting is considered here as plastic deformation of material induced by taking advantage of thermal expansion phenomenon, without use of external forces. Effect of thermal upsetting has been applied since long ago for changing shape of metal objects by heating with a flame [1], [2], [3].

Thermal deformations can be produced with many heat sources, yet controlled inducing of thermal stresses and permanent strain requires application of a tool, which provides local heat input into the workpiece, is well and easily controlled, and can operate in industrial environment. Among different heat sources the laser beam exhibits outstanding features with respect to controllability in space and time. It represents well-defined heat flux, which can be applied accurately to the demanded surface area of the object, is maneuverable, propagates both through atmospheric air and vacuum, can be delivered at a distance, into locations difficult to access otherwise, through the windows into closed chambers, containers or vessels, both in macro and micro scale.

Alignment and adjustment procedures in manufacturing technology present large area of potential and already successful applications of one of thermal forming methods - the laser forming method. Adjustment with the use of a laser beam, compared to traditional forming and positioning techniques, offers high accuracy and short operation time due to the lack of mechanical contact between tool and the adjustment object. Flexibility of the method allows alignment of miniature electric, electronic, mechanical and optic components, a few millimeters in size, with accuracy in the sub-micron or sub-milliradian range [4], [5], [6], [7], [8]. Unavoidable influence of scattering of material properties and geometric dimensions on thermal forming effects is accounted for and reduced using closed-loop control of adjustment process.

Movement and/or pulsed application of heat energy allows creating steep thermal gradients, which produce high thermal stresses necessary to achieve thermal upsetting. All three mechanisms described in the literature on laser forming method [9] involve thermal upsetting. The Temperature Gradient Mechanism requires steep thermal gradient across material thickness, while the Upsetting Mechanism necessitates high temperature gradient and sufficient constraint in the plane of material. The Buckling Mechanism similarly acts due to in-plane temperature gradient and constraint, but thermal upsetting is produced in post-critical state of the heated object.

Accurate assembly and alignment of micro parts is accomplished using structures called actuators. Their deformation produced by heating with a laser beam can be used to adjust, calibrate or trim critical dimensions and functional characteristics of components. So-called two-bridge layout is a basic constituent used in various designs of actuators.

Modelling of actuators allows for improvement of their designs. It opens possibilities of creating desired characteristics through the design optimisation. Thermo-mechanical behavior of actuators dedicated to adjustment application was investigated mainly experimentally and using Finite Element Method [4], [5], [10], [11].

Presented analysis addresses the two-bridge actuator and its deformation induced thermally without remelting of material, i.e. in solid state. Analytic-numerical model is developed to describe thermo-elastic-plastic deformation of the actuator as a miniature frame structure under local thermal load.

2 Experiments

Samples made of a low-carbon steel were irradiated with a stationary Nd:YAG laser beam (**figure 1**). The RSY 150 Q laser operated in the continuous wave (cw) mode, producing a beam of a nearly uniform (top-hat) power intensity on its circular cross-section.

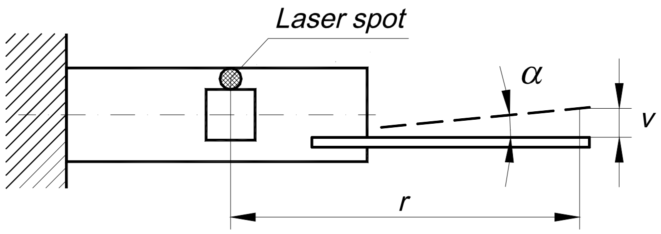

Figure 1: Local heating of specimen and non-contact measurement of its angular deformation.

Specimens of dimensions 80 x 10 x 0.815 mm with rectangular opening 6 x 6 mm cut out by blanking were annealed in a furnace at 400 °C prior to laser heating. Annealing produced oxide layer which provided stable conditions of the beam energy absorption.

Transient and permanent angular deformation of samples was measured by a non-contact method using Laser Scan Micrometer LS-3100/3034 (Keyence Co., Japan). Additional lightweight element of good surface quality was attached to the sample in order to enhance precision of displacement measurements. Angle α used as a measure of thermally induced deformation of the sample was calculated from the measured displacement v and radius r (**figure 1**) as $\alpha = \arctan(v/r)$. The angular deformation α of the sample is considered positive when the right part of the sample moves up, as shown in **figure 1**.

An example of the time run of the angular deformation $\alpha(t)$ is presented in **figure 2**. During the heating phase the sample deforms with the negative value of angle α due to thermal expansion of the heated region. When the heat source is switched off, the cooling phase starts. Depending on applied processing parameters two types of behavior of the structure can be observed: (1) return to the initial form (thermo-elastic deformation) or (2) a small change of the form occurs (thermo-elastic-plastic deformation), like in **figure 2**.

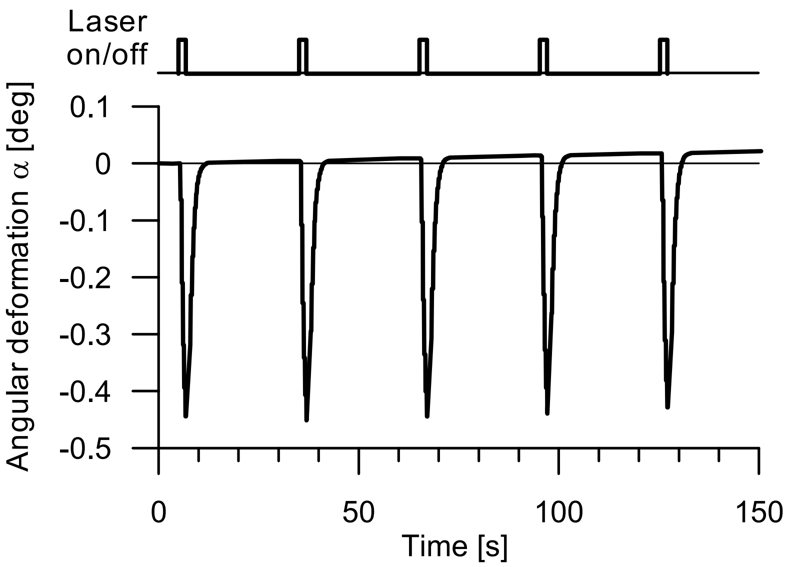

Figure 2: Time run of the angular deformation $\alpha(t)$ during experiment with 5 irradiations of power 43.4 W and heating time 1.8 s.

An example of the residual plastic angular deformation, i.e. value of the angle α after each heating and cooling cycle, for the process presented in **figure 2**, is shown in **figure 3**. The characteristics has degressive course with tendency to saturation for greater numbers of irradiations. Presented analysis addresses thermally induced deformation produced during the initial irradiation applied to the stress-free specimen.

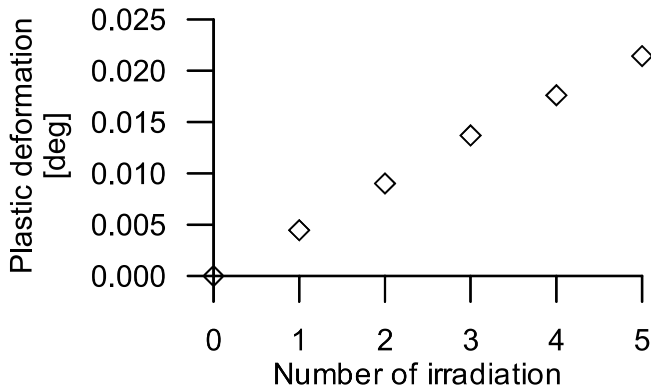

Figure 3: Residual angular deformation produced in a sequence of 5 irradiations of power 43.4 W and heating time 1.8 s.

3 Theoretical model

Taking into account low temperature rate and strain rate the considered thermo-mechanical problem can be treated as uncoupled and quasi-static one because the inertia effects may be neglected as well as the influence of strain on the temperature field. Therefore the heat transfer analysis will be done first and then the quasi-static analysis of the structure behaviour will be performed using already defined temperature distribution.

The considered structure is regarded as a miniature frame structure and can be divided into four segments (**figure 4**):

- segments **1** and **2**: beams subject to longitudinal and bending deformation,
- segments **3** and **4**: plates - components much more stiff to deformation in comparison with beams **1** and **2**, and considered as rigid.

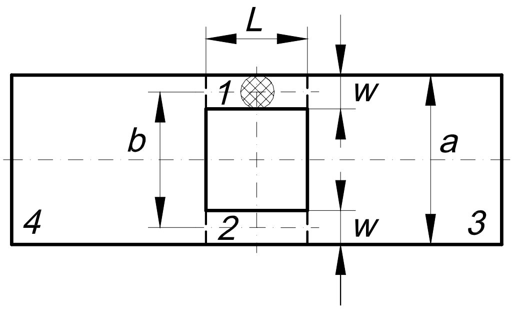

Figure 4: Division of the structure into segments.

3.1 Temperature field

Laser beam spot diameter is assumed equal to the width of the heated segment **1**. Rough estimate of the heat power transferred in segment **1** by conduction and its comparison with heat power absorbed by the material suggest that convective and radiation losses contribute little to the total heat transfer for the interesting processing parameters range [12]. This observation and final results of the analysis justify assumption of the one-dimensional heat flow in a part of segment **1**. While this assumption cannot be defended for a region adjacent to the laser beam spot, it may be used for the rest of heated segment, according to the Saint-Venant's principle in heat conduction problems [13].

A model of the heat transfer in segment **1** applied in the analysis is illustrated by **figure 5**. Heat absorbed by the material is divided into two equal parts, which are transferred by conduction towards both ends of segment **1**.

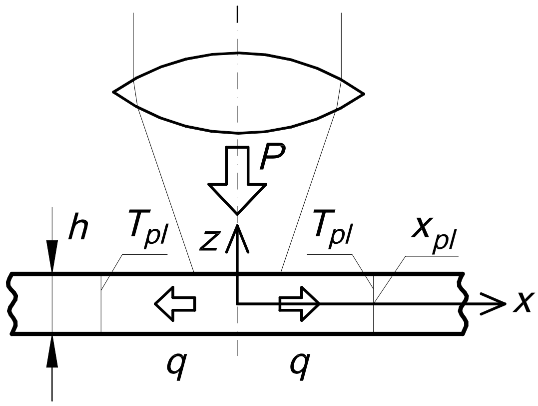

Figure 5: Schematic of the heat transfer model in segment **1.**

Increase of temperature above the initial temperature in the one dimensional heat flow caused by a heat flux q acting constantly during time of heating t_h is described by the following linear thermo-elasticity solution [14]

$$\Delta T(x,t) = \frac{2q}{\lambda}\left[\sqrt{\kappa t}\ ierfc\left(\frac{x}{2\sqrt{\kappa t}}\right) - \sqrt{\kappa(t-t_h)}\ ierfc\left(\frac{x}{2\sqrt{\kappa(t-t_h)}}\right)\right] \quad (1)$$

where the heat flux q is calculated in the considered problem as

$$q = \frac{AP}{2S} \quad (2)$$

and A is the absorption coefficient; P is the laser beam power; $\kappa = \frac{\lambda}{\rho c}$ is the thermal diffusivity; λ is the thermal conductivity; ρ is the density; c is the specific heat of the material; S is the cross-sectional area of the segment; $S = wh$; w is the width of segment **1**; h is the thickness of material **(figure 5**); t is time. First term in square brackets of equation (1) describes heating phase ($t \le t_h$), while the second term contributes to the temperature distribution after stopping the action of heat flux q.

Solution (1) is based on constant material data values assumption, irrespective of material temperature. Dependence of material data on temperature will be respected throughout presented analysis by applying the data for the mean temperature of the process under consideration. The following material data were used in analytic and numerical calculations: $A = 0.88$, the coefficient of linear thermal expansion $\alpha_T = 14.6 \cdot 10^{-6}$ [1/K], $\lambda = 38$ [W/(m K)], $c = 625$ [J/(kg K)], $\rho = 7680$ [kg/m^3] [12]. These values are within ranges recommended in [15] for mild steel in processes of the mean temperature 500÷600 °C.

A diagram illustrating development of temperature field according to formula (1) in one half of segment **1** is presented in **figure 6**.

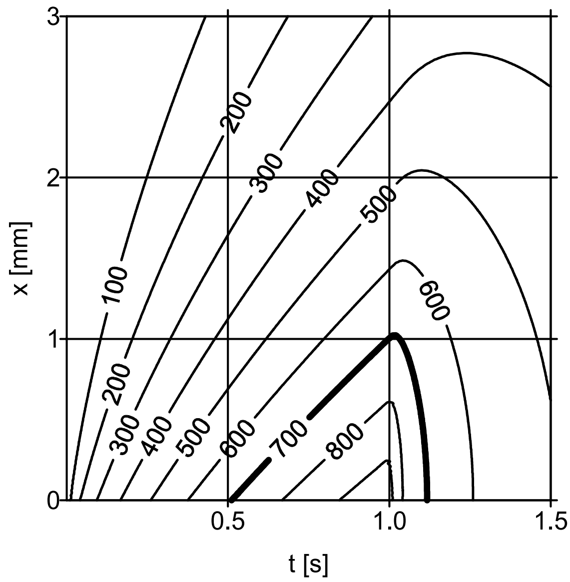

Figure 6: A contour map of the temperature increase $\Delta T(x,t)$ in one half of segment **1** for laser beam power 43.4 W, heating time 1 s and low-carbon steel material.

Maximal increase in material temperature according to solution (1) occurs in the middle section ($x = 0$) and can be expressed during heating phase as

$$\Delta T_{\max} = \frac{AP}{\rho c S}\sqrt{\frac{t}{\pi\kappa}} \tag{3}$$

3.2 Thermal elongation

The increase ΔL_1^T of length of segment **1** due to the phenomenon of thermal expansion and temperature change is described by formula

$$\Delta L_1^T = 2\int_0^{L/2} \alpha_T \, \Delta T(x,t)\, dx \tag{4}$$

where: L is the initial length of segments **1** and **2**.

Assuming value of the thermal expansion coefficient α_T not dependent on temperature, and using formula (1) the increase ΔL_1^T of length at time $t \le t_h$ is expressed as

$$\Delta L_1^T = \frac{4\alpha_T\, q\sqrt{\kappa\, t}}{\lambda}\int_0^{L/2} ierfc\left(\frac{x}{2\sqrt{\kappa\, t}}\right)dx \tag{5}$$

The above expression contains integral of the ierfc function. The repeated integral of the complementary error function derived by integrating by parts is

$$i^2 erfc(x) \equiv \int_x^{\infty} ierfc(u)du = \frac{1}{4}\left[erfc(x) - 2x\, ierfc(x)\right] \tag{6}$$

Performing substitution of variables and suitable change of the upper integral limit we obtain

$$\int_0^{m} ierfc(u)\, du = \frac{1}{4}\left[erf(m) + 2m\, ierfc(m)\right] \tag{7}$$

Thermal elongation of the heated segment **1**, derived using formulae (2), (5) and (7) for $t \le t_h$ is described by the following formula

$$\Delta L_1^T = \frac{AP\alpha_T\, t}{\rho\, c\, S}\left[erf\left(\frac{L}{4\sqrt{\kappa\, t}}\right) + \frac{L}{2\sqrt{\kappa\, t}}\, ierfc\left(\frac{L}{4\sqrt{\kappa\, t}}\right)\right] \tag{8}$$

This increase of length of segment **1** due to local temperature change is the cause of thermal stresses to occur in the structure.

3.3 Internal forces

Thermal buckling phenomenon will not be accounted for in the analysis as unlikely in conditions of small slenderness ratio of the heated beam and weak axial restraint, which will be proved later. The Bernoulli-Euler assumption about beam sections that remain plane and perpendicular to the axis after loading and that effect of lateral contraction may be neglected will be employed.

A scheme for the static analysis of the structure is shown in **figure 7.**

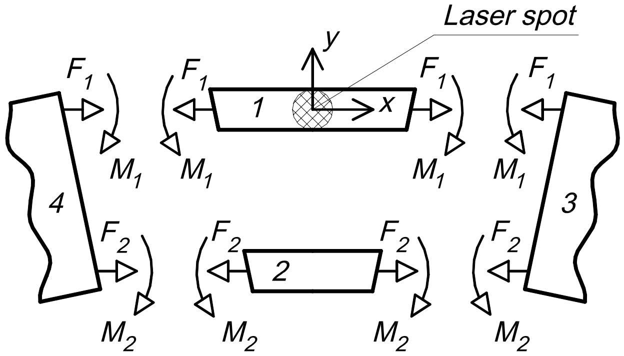

Figure 7: Denotation and directions assigned to positive values of internal forces and moments of forces acting on respective segments of the structure.

From equilibrium conditions result the following relations between internal forces

$$F_2 = -F_1 \tag{9}$$

$$M_2 = F_2 b - M_1 \tag{10}$$

where $b = a - w$ is the distance between longitudinal axes of segments **1** and **2** (**figure 4**).

Changes of lengths of segments **1** and **2** due to longitudinal forces are

$$\Delta L_1^F = \frac{F_1 L}{k_F} \quad ; \quad \Delta L_2^F = \frac{F_2 L}{k_F} \tag{11}$$

where: $k_F = ES$ is the longitudinal rigidity of segments **1** and **2**; E is the Young's modulus.

Lengths L_1 and L_2 of segments **1** and **2**, respectively, result from the initial value L and changes due to the temperature change and existence of internal forces

$$L_1 = L + \Delta L_1^T + \Delta L_1^F \quad ; \quad L_2 = L + \Delta L_2^F \tag{12}$$

Effect of temperature change in segment **2** was omitted in the above formula as negligible.

Bending deformation of segments **1** and **2** expressed by the angle of rotation β at ends of segments can be estimated using the pure bending theory as

$$\beta = \frac{M_1 L}{2k_M} = \frac{M_2 L}{2k_M} \tag{13}$$

where: $k_M = EJ_z$ is the bending rigidity of segments **1** and **2**; $J_z = \frac{hw^3}{12}$ is the moment of inertia of the rectangular cross-sections of segments **1** and **2** about central axes parallel to axis z.

From equations (13) we obtain

$$M_1 = M_2 \tag{14}$$

For small deformations of the structure the following approximation may be employed

$$\beta \approx tg\beta = \frac{L_1 - L_2}{2b} \tag{15}$$

The angle of rotation β is related to the angle of deformation α of the structure according to formula

$$\alpha = -2\beta \tag{16}$$

From equilibrium conditions, deformation and geometric relations result the following formulae for internal forces and angular deformation of the structure in elastic state

$$M_1 = \frac{b k_M k_F}{L(b^2 k_F + 4k_M)} \Delta L_1^T \tag{17}$$

$$F_1 = -\frac{2k_M k_F}{L(b^2 k_F + 4k_M)} \Delta L_1^T \tag{18}$$

$$\alpha = -\frac{b k_F}{b^2 k_F + 4k_M} \Delta L_1^T \tag{19}$$

Internal forces and angular deformation of the considered frame structure under thermal loading are described in elastic state as functions of thermal elongation ΔL_1^T. Applying already derived expression (8) for thermal elongation ΔL_1^T in equation (19) we arrive at a formula for the thermo-elastic angular deformation $\alpha_{el}(t)$ [rd] of the structure during heating phase ($t \leq t_h$)

$$\alpha_{el}(t) = -\frac{3AP\alpha_T bt}{\rho c h w\,(3b^2 + w^2)} \left[erf\left(\frac{L}{4\sqrt{\kappa t}}\right) + \frac{L}{2\sqrt{\kappa t}} ierfc\left(\frac{L}{4\sqrt{\kappa t}}\right) \right] \tag{20}$$

The above purely analytic formula describes thermo-elastic angular deformation of the structure under consideration, dependent on thermal processing, material and geometric parameters.

3.4 Plastic deformation

With increasing temperature thermal stresses in the heated segment **1** increase and the yield stress of the material declines. Compressive force can thus produce material upsetting. Plastic strain produced during thermal upsetting will be calculated using the critical temperature concept applied in the inherent strain method [16].

Watanabe and Satoh [16] defined the critical temperature as "the temperature value above which material does not resist to deformation". Jang, Seo and Ko [17] described it as the temperature "at which strength of material becomes negligible". Similarly Anderson [18] says about temperature "at which material strength has decreased significantly" and "material properties such as yield stress and Young's modulus become negligible". Andersen [19] calls this temperature "mechanical melting point over which yield stresses disappear".

Dependence of yield stress on temperature for low-carbon and medium-carbon steels is shown in **figure 8.** For the purpose of presented here analysis the critical temperature T_{pl} is assumed the temperature at which material yield stress value is regarded negligible, and its value taken as 720 °C.

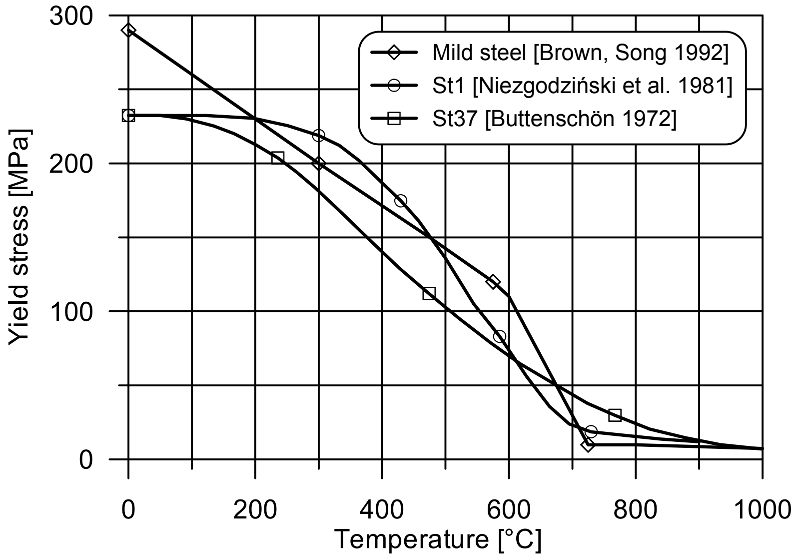

Figure 8: Yield stress dependence on temperature for low- and medium-carbon steels [20], [21], [22].

Jang, Seo and Ko [17] assumed $T_{pl} = 870$ °C for mild steel. Anderson [18] applied $T_{pl} = 660$ °C. Yu et al. [23] used $T_{pl} = 500$ °C also for mild steel, but they noted that for this material Young's modulus and yield stress become very small at a temperature above 725 °C. Taking into account the initial temperature T_0 = 20 °C, the line indicating $\Delta T(x,t) = 700$ °C in **figure 6** corresponds to the momentary position of the critical temperature isotherm $T_{pl} = 720\,°$C.

Restraint of the heated segment **1** due to reaction of the rest of the structure can be characterised by the restraint rigidity coefficient (constraint ratio) R [24], which by definition relates thermal strain $\varepsilon^T = \alpha_T \Delta T$ to the strain ε^F due to forces as

$$R = -\frac{\varepsilon^F}{\varepsilon^T} \tag{21}$$

Strain ε_1^F of segment **1** due to axial force F_1 may be calculated in the elastic state as

$$\varepsilon_1^F = \frac{F_1}{ES} \tag{22}$$

Temperature in the locally heated segment **1** varies along its axis, with distribution described by equation (1). However if we calculate mean thermal strain of segment **1** as

$$\varepsilon_1^T = \frac{\Delta L_1^T}{L} \tag{23}$$

then using formula (18) the restraint rigidity coefficient for the whole segment **1** can be derived as

$$R_1 = \frac{w^2}{2(3b^2 + w^2)} \tag{24}$$

For the samples considered here $R_1 = \frac{1}{98}$. It should be noticed that the restraint rigidity coefficient R (21) varies for individual material sections along segment **1** according to the temperature distribution.

Stress $\sigma_1^F = F_1 / S$ resulting from the existence of force F_1 in segment **1** can be expressed using (8), (18) and (24) as

$$\sigma_1^F = -R_1 \frac{APE\alpha_T t}{\rho c L S}\left[erf\left(\frac{L}{4\sqrt{\kappa t}}\right) + \frac{L}{2\sqrt{\kappa t}}\, ierfc\left(\frac{L}{4\sqrt{\kappa t}}\right)\right] \tag{25}$$

or using (3)

$$\sigma_1^F = -R_1 E\alpha_T \Delta T_{\max} \frac{\sqrt{\pi\kappa t}}{L}\left[erf\left(\frac{L}{4\sqrt{\kappa t}}\right) + \frac{L}{2\sqrt{\kappa t}}\, ierfc\left(\frac{L}{4\sqrt{\kappa t}}\right)\right] \tag{26}$$

Let us note that stress induced by local heating of a bar with ends rigidly clamped (**figure 9a**) may be derived using formula (8) as

$$\sigma_a = -E\alpha_T \Delta T_{\max} \frac{\sqrt{\pi\kappa t}}{L}\left[erf\left(\frac{L}{4\sqrt{\kappa t}}\right) + \frac{L}{2\sqrt{\kappa t}}\, ierfc\left(\frac{L}{4\sqrt{\kappa t}}\right)\right] \tag{27}$$

and for a clamped at both ends and uniformly heated bar (**figure 9b**) thermal stress is

$$\sigma_b = -E\alpha_T \Delta T \tag{28}$$

and $R = 1$.

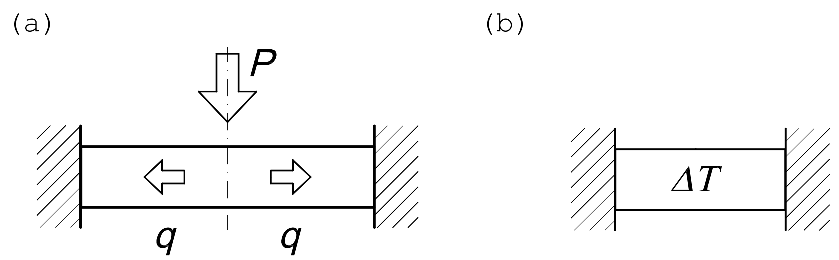

Figure 9: Bar rigidly clamped and heated: (a) locally, (b) uniformly.

Therefore stress σ_1^F due force F_1 may be expressed as

$$\sigma_1^F = R_1 \sigma_a \tag{29}$$

Equations (25) – (29) clearly show role of uniform heating, local heating and restraint in generation of thermal stress in relevant problems.

Figure 10 shows approximate yield stress dependence on material temperature and dependence of stress σ_1^F on maximal temperature $T_{\max} = \Delta T_{\max} + T_0$ in segment **1** during heating phase, and up to the yield limit. Dashed line represents thermal stress σ_b.

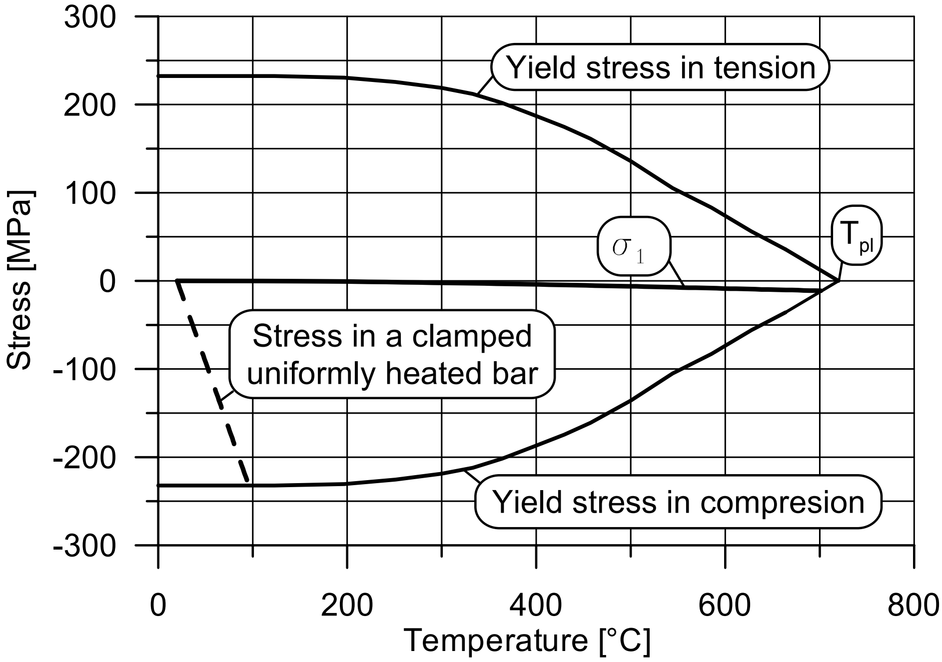

Figure 10: Effect of restraint on stress due to axial force in segment **1** and in a clamped bar during heating.

The figure illustrates strong influence of the heated element restraint on induced thermal stresses. Small value of the restraint rigidity coefficient in case considered here implies that thermal upsetting will start at temperature value close to the critical temperature T_{pl}.

The following reasoning may be employed in calculating plastic strain. If temperature $T(x,t) = T_0 + \Delta T(x,t)$ within certain region of segment **1** is equal or greater than the material critical temperature T_{pl}, then, due to negligible yield stress value at this temperature, the stress σ_1^F undergoes relaxation.

Consequently, elastic strain related to stress σ_1^F is converted into plastic strain of material upsetting

$$\varepsilon_{pl} = \frac{\sigma_1^F}{E} \tag{30}$$

Let us note that using formula (25) in the above equation, the Young's modulus is eliminated and under applied assumptions does not enter calculation of thermal deformations, neither elastic, nor plastic.

Change of length of segment **1** due to the plastic deformation is

$$\Delta L_1^{pl} = 2\varepsilon_{pl} x_{pl} \tag{31}$$

where x_{pl} is the maximal extent of the critical temperature T_{pl}.

The maximal extent x_{pl} of the critical isotherm is slightly greater then its range at the end of heating phase ($t = t_h$), as is shown in **figure 6**. This slight increase of the critical isotherm extent will be neglected for its little influence on final results regarding thermally induced deformation. Under this approximation the value of extent x_{pl} of the critical temperature T_{pl} satisfies the following equation

$$T_{pl} - T_0 = \frac{2q}{\lambda}\sqrt{\kappa t_h}\; ierfc\left(\frac{x_{pl}}{2\sqrt{\kappa t_h}}\right) \tag{32}$$

The bisection algorithm has been applied in numerical calculating value of x_{pl} from equation (32).

If we apply material upsetting expressed by plastic deformation ΔL_1^{pl} in place of ΔL_1^T in equation (19), then we are able to calculate the angular plastic deformation α_{pl} [rd] of the structure

$$\alpha_{pl} = -\frac{b k_F}{b^2 k_F + 4k_M}\Delta L_1^{pl} \tag{33}$$

and using formulae (8), (18), (30) and (31) we obtain the following formula

$$\alpha_{pl} = R_1^2 \frac{12 A P \alpha_T b x_{pl} t_h}{\rho c L S w^2}\left[erf\left(\frac{L}{4\sqrt{\kappa t_h}}\right) + \frac{L}{2\sqrt{\kappa t_h}} ierfc\left(\frac{L}{4\sqrt{\kappa t_h}}\right)\right] \tag{34}$$

Plastic angular deformation of the considered frame structure is directly proportional to the square of the restraint rigidity coefficient R_1, what emphasises the influence of geometric parameters on behaviour of the structure.

The threshold processing parameters for producing plastic deformation result from the condition of raising material temperature to the critical temperature value T_{pl}.

$$\Delta T_{\max} + T_0 = T_{pl} \tag{35}$$

From equation (3) result two alternative formulae for the threshold laser beam power P_{pl} and threshold time of heating t_{pl}

$$P_{pl} = \frac{\sqrt{\pi}\lambda S(T_{pl} - T_0)}{A\sqrt{\kappa t_h}} \quad ; \quad t_{pl} = \frac{\pi}{\kappa}\left(\frac{\lambda S(T_{pl} - T_0)}{AP}\right)^2 \tag{36}$$

4 Results

Theoretical dependence of the threshold time of heating t_{pl} on the applied laser beam power P for producing material upsetting in the considered frame structure is shown in **figure 11.**

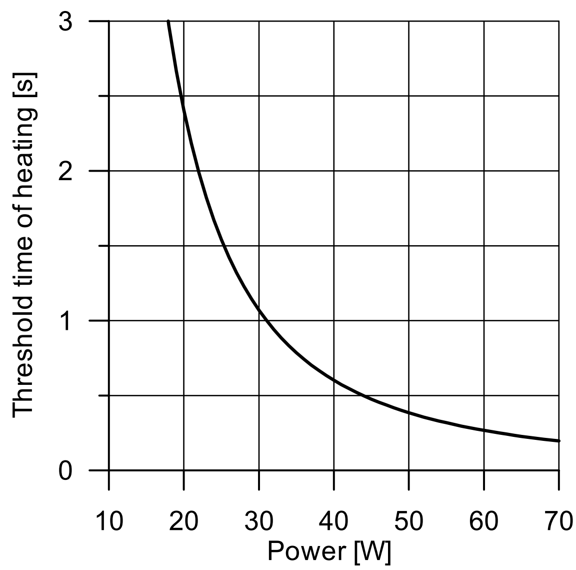

Figure 11: Threshold time of heating dependent on the applied laser beam power.

Comparison of analytic solution (20) for thermo-elastic angular deformation α_{el} of the structure and values measured in experiments is presented in **figure 12.** Experimental points in **figure 12** correspond to the extreme negative angular deformations measured during heating phase, such that can be seen in **figure 2.** Validity of the analytic solution (20), limited to the elastic state, is shown by continuous lines **figure 12,** for several levels of applied laser beam power. Beyond the threshold time of heating t_{pl} plastic deformation develops. This fact is reflected by the increasing deflections of experimental points from theoretical predictions calculated for a perfectly elastic behavior and marked by dashed lines. In the case of low power values and long heating time the dissipation of heat by convection and radiation has greater share in total heat transfer balance and significantly influences temperature field, as well as thermally induced deformation. This fact can explain considerable difference between theoretical and experimental results for laser power $P = 20$ W and long heating time.

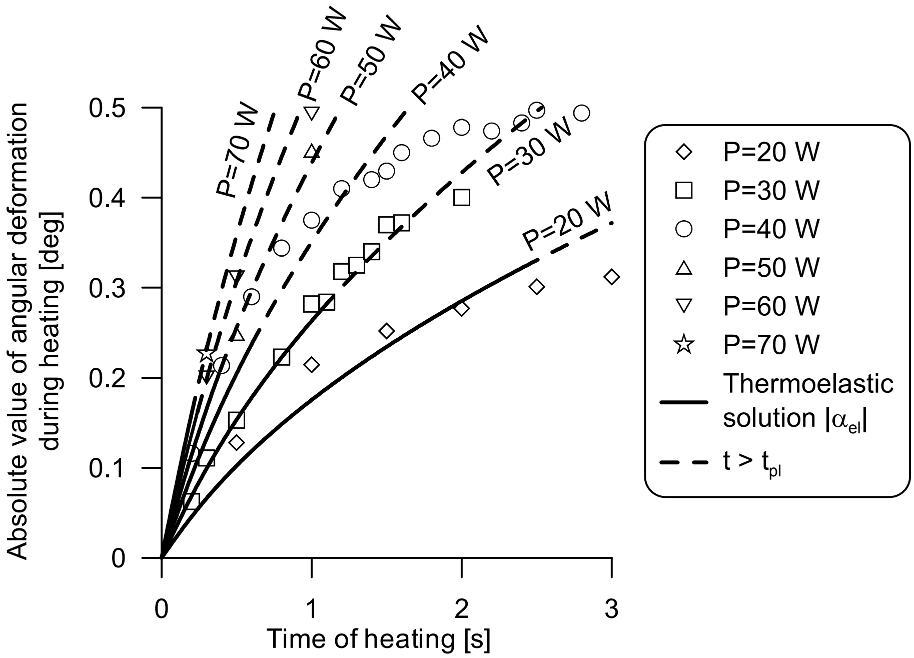

Figure 12: Experimental and analytic results for angular deformation during heating.

Experimental results and analytic-numerical solution (34) for plastic angular deformation α_{pl} are presented in **figure 13.**

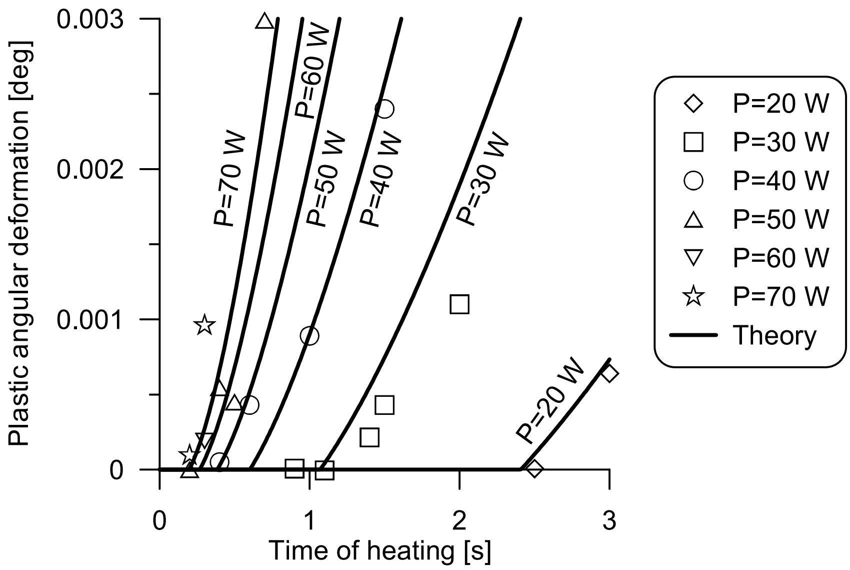

Figure 13: Experimental and theoretical results for plastic angular deformation.

It should be noted that angle α_{pl} represents only plastic component of deformation, while experimental values reflect also elastic residual strain of the structure.

All presented theoretical results were calculated using the same set of material data values. More accurate calculations should take into consideration different mean temperature of the process for different power levels and heating times. Some contribution to discrepancies between calculated and measured values could have the use of a mechanical laser beam shutter in experiments (because of failure of the acousto-optical Q-switch) and its low accuracy of setting time of heating.

Theoretical predictions agree in general with experimental results. Taking into account simplifications employed for the theoretical model, in particular assumed one-dimensional temperature distribution in the vicinity of laser spot and negligence of heat dissipation by convection and radiation, presented model yields reasonable estimates of thermo-elastic and thermo-plastic deformations, as well as threshold processing parameters.

5 Conclusions

Successful application of micro adjustment by use of actuators and thermal upsetting effect necessitates careful design of suitable component structures. Among different modelling methods, including physical modelling and Finite Element Method simulations, analytical modelling, if successfully accomplished, gives best understanding of the role of particular processing and material parameters in considered problems.

In spite of application of a simple, one-dimensional heat transfer model presented analysis gives insight into thermo-elastic-plastic behaviour of the considered frame structure and allows quantitative description of induced deformations. Use of the restraint rigidity coefficient in the model facilitates theoretical description and highlights fundamental role of constraint in thermal upsetting.

Derived formulae can be applied in optimization of actuators and similar frame structures of micro-, as well as macro-scale. The model can be adapted to sources of heat other than laser beam.

6 Acknowledgement

The work was done partly in the frame of activities of the Centre of Excellence for Laser Processing and Material Advanced Testing LAPROMAT, founded by the European Union.

7 References

[1] Holt J., Contraction as a Friend in Need, Joseph Holt 1938 (see [3])

[2] Holt R. E., Flame Straightening Basics. Welding Engineer, Sept. 1965, 49-53.

[3] Holt R. E., Primary Concepts for Flame Bending. Welding Journal, June 1971, 416-424.

[4] Hoving W., Verhoeven E. C. M., High-precision micro-assembly using laser-adjustment. Laser in der Elektronikproduktion & Feinwerktechnik - LEF 2000. Geiger M., Otto A. (eds.), Meisenbach Bamberg, 2000, 165-174.

[5] Huber A., Müller B., Meyer-Pittroff F., Laserstrahljustieren als Innovation für die Montage von Mikrosystemen. Vollertsen F., Kleiner M. (eds.), Idee - Vision – Innovation, Meisenbach, Bamberg, 2001, 275-286.

[6] Kitada K., Asahi N., Laser adjustment of beryllium copper sheet using temperature gradient mechanism. Third International Symposium on Laser Precision Microfabrication. Miyamoto I., Kobayashi K. F., Sugioka K., Poprawe R., Helvajian H. (eds.), Proceedings of the SPIE, Volume 4830, 2003, 30-35.

[7] Esser G., Schmidt M., Dirscherl M., Laser adjustable actuators for high-accuracy positioning of micro components. Fourth International Symposium on Laser Precision Microfabrication. Miyamoto I., Ostendorf A., Sugioka K., Helvajian H. (eds.), Proceedings of the SPIE, Volume 5063, 2003, 177-182.

[8] Matsushita N., Laser micro-bending for precise micro-fabrication of magnetic disk drive components. Fourth International Symposium on Laser Precision Microfabrication. Miyamoto I., Ostendorf A., Sugioka K., Helvajian H. (eds.), Proceedings of the SPIE, Volume 5063, 2003, 24-29.

[9] Vollertsen F., Mechanisms and Models for Laser Forming. Proceedings of the 26th International CIRP Seminar on Manufacturing Systems - LANE '94 (Laser Assisted Net Shape Engineering), Geiger M., Vollertsen F. (eds.), Meisenbach-Verlag, Bamberg, 1994, 345-360.

[10] Müller B., Huber A., Geiger M., Sub-Micron Accuracy of Assembled Systems by Laser Adjustment. Proc. of 6th Int. Conf. Tech. Plasticity (ICTP), 1999, 1037-1042.

[11] Olowinsky A. M., Bosse L., Laser beam micro forming as a new adjustment technology using dedicated actuator structures. Smart Sensors, Actuators, and MEMS. Chiao J.-C., Varadan V. K., Cane C. (eds.), Proceedings of the SPIE, Volume 5116, 2003, 285-294.

[12] Widłaszewski J., Modelling of actuators for adjustment with a laser beam. Proceedings of the Laser Assisted Net Shape Engineering 4, Geiger M., Otto A. (eds.), Meisenbach-Verlag Bamberg 2004, Vol. 2, 1083-1094.

[13] Boley B. A., Weiner J. H., Theory of thermal stresses. John Wiley & Sons, Inc., 1960.

[14] Carslaw H. S., Jaeger J. C., Conduction of Heat in Solids. Oxford University Press, 1946.

[15] Frolov W. W., Vinokurov V. A., Volczenko W. N., Parachin W. A., Arutionowa I. A., Theoretical foundations of welding. High School Publishing House, Moscow 1970 (in Russian).

[16] Watanabe M., Satoh K., Effect of Welding Conditions on the Shrinkage Distortion in Welded Structures. The Welding Journal, Welding Research Supplement 40 (1961) 8, 377-384.

[17] Jang C. D., Seo S. I., Ko D. E., A Study on the Prediction of Deformations of Plates Due to Line Heating Using a Simplified Thermal Elastoplastic Analysis, Journal of Ship Production, Vol. 13, No. 1, 1997, 22-27.

[18] Anderson R. J., Experiments and simulation of line heating of plates. Master of Sciences Thesis, Massachusetts Institute of Technology, 1999.

[19] Andersen M. R., Fatigue Crack Initiation and Growth in Ship Structures. Ph. D. Thesis. Technical University of Denmark, 1998.

[20] Brown S., Song H., Finite element simulation of welding of large structures. Journal of Engineering for Industry. 114(4):441-451, November 1992 (see [18]).

[21] Niezgodziński M. E., Niezgodziński T., Strength of Materials. PWN, Warsaw 1981 (in Polish).

[22] Buttenschön K., Beulen von dünnwandigen Kastenträgern aufgrund von Schweißeigenspannungen. Schweiß. u. Schneid. 24 (1972) no. 6, 217-221 (see [25]).

[23] Yu G., Anderson R. J., Maekawa T., Patrikalakis N. M., Efficient Simulation of Shell Forming by Line Heating.

International Journal of Mechanical Sciences. Vol. 43, No. 10, 2349-2370, October 2001.

[24] Taira S., Ohtani R., Theory of high-temperature strength of materials. Metallurgy, Moscow, 1986 (in Russian).

[25] Radaj D., Heat Effects of Welding. Springer-Verlag, 1992.